Hemodynamic Response of the Three Macular Capillary Plexuses in Dark Adaptation and Flicker Stimulation Using Optical Coherence Tomography Angiography

Peter L. Nesper,[1] Hee Eun Lee,[1] Alaa E. Fayed,[1,2] Gregory W. Schwartz,[1,3,4] Fei Yu,[5] and Amani A. Fawzi[1]

[1]Department of Ophthalmology, Feinberg School of Medicine, Northwestern University, Chicago, Illinois, United States
[2]Department of Ophthalmology, Kasr Al-Ainy School of Medicine, Cairo University, Cairo, Egypt
[3]Department of Physiology, Feinberg School of Medicine, Northwestern University, Chicago, Illinois, United States
[4]Department of Neurobiology, Weinberg College of Arts and Sciences, Northwestern University, Chicago, Illinois, United States
[5]Department of Biostatistics, Fielding School of Public Health, University of California-Los Angeles, Los Angeles, California, United States

Correspondence: Amani Fawzi, Department of Ophthalmology, Feinberg School of Medicine, Northwestern University, 645 North Michigan Avenue, Suite 440, Chicago, IL 60611, USA; afawzimd@gmail.com.

Submitted: August 8, 2018
Accepted: January 14, 2019

Citation: Nesper PL, Lee HE, Fayed AE, Schwartz GW, Yu F, Fawzi AA. Hemodynamic response of the three macular capillary plexuses in dark adaptation and flicker stimulation using optical coherence tomography angiography. *Invest Ophthalmol Vis Sci*. 2019;60:694–703. https://doi.org/10.1167/iovs.18-25478

Purpose. To assess retinal microvascular reactivity during dark adaptation and the transition to ambient light and after flicker stimulation using optical coherence tomography angiography (OCTA).

Methods. Fifteen eyes of 15 healthy participants were dark adapted for 45 minutes followed by OCTA imaging in the dark-adapted state. After 5 minutes of normal lighting, subjects underwent OCTA imaging. Participants were then subjected to a flashing light-emitting diode (LED) light and repeat OCTA. Parafoveal vessel density and adjusted flow index (AFI) were calculated for superficial (SCP), middle (MCP), and deep capillary plexuses (DCP), and then compared between conditions after adjusting for age, refractive error, and scan quality. SCP vessel length density (VLD) was also evaluated. Between-condition capillary images were aligned and subtracted to identify differences. We then analyzed images from 10 healthy subjects during the transition from dark adaptation to ambient light.

Results. SCP vessel density was significantly higher while SCP VLD was significantly lower during ambient light and flicker compared to dark adaptation. There was a significant positive mean value for DCP "flicker minus dark or light," suggesting more visible vessels during flicker due to changes in flow, dilation, or vessel recruitment. We found a significant, transient increase in SCP and decrease in both MCP and DCP vessel density during the transition from dark to light.

Conclusions. We show evidence suggesting constriction of deeper vessels and dilation of large SCP vessels during the transition from dark to light. This contrasts to redistribution of blood flow to deeper layers during dark adaptation and flicker stimulation.

Keywords: optical coherence tomography angiography, OCT, neurovascular coupling, dark adaptation, flicker stimulation

Retinal blood flow, as in the rest of the brain, is actively regulated in response to neuronal activity.[1,2] Impairment of this coupling mechanism in the retina is commonly encountered during microvascular pathologies, such as diabetic retinopathy.[3,4] Currently, there are limited studies (and technologies) that explore the human retinal capillary responses during neurovascular coupling, a key to understanding the pathological disruption during disease.

The photoreceptor inner segments have the highest metabolic demand of any retinal layer in the dark.[5] The most intensive photoreceptor demand occurs during dark adaptation, which in the absence of autoregulation of the choroidal vasculature,[6] is partially met by diffusion from the retinal vasculature.[7,8] Early ultrasound and laser Doppler studies found increased blood velocity in major arteries during dark adaptation in the human retina,[9,10] as well as increased diameter and blood flow velocity in major veins.[11] This was attributed to neurovascular coupling to support the increased oxygen demand of the dark-adapted photoreceptors. Later, several studies using infrared reflectance or scanning laser ophthalmoscopy and retinal vessel analyzers reported no significant increase in large vessel diameters during dark adaptation in humans.[12–14] Another study used a laser Doppler flow meter and found no change in blood flow during dark adaptation, but instead recorded a transient increase in retinal blood velocity following transition from dark adaptation to light.[15]

Flicker stimulation studies have produced more consistent results, perhaps in part because flicker leads to neural activation in the inner retina, where most previous hemodynamic studies have focused. Flicker-induced arterial and venular vasodilation and increased blood flow velocity have been reported in humans and rodents.[16–26] The techniques used to study the vascular response to dark adaptation and flicker

stimulation in humans have largely been limited to large vessels. Moreover, they lack the necessary axial resolution to differentiate individual capillary plexuses. Histologic studies have confirmed the presence of the superficial (SCP), middle (MCP), and deep capillary plexuses (DCP) in the human macula.[27]

Optical coherence tomography angiography (OCTA) is a noninvasive technique capable of acquiring high-resolution, depth-resolved images in a matter of seconds, resolving motion of blood cells in capillaries and major vessels with sufficient depth resolution to image the three capillary networks and their connectivity.[28–30] OCTA also uses infrared light, allowing imaging of the dark-adapted retina without disrupting dark adaptation. One previous OCTA study performed full-thickness (non-depth resolved) retinal capillary measurements and found an increase in parafoveal flow index (indirect, relative velocity measure) in human subjects during checkerboard pattern stimulation.[31] In order to better characterize the response in each capillary plexus, we performed OCTA imaging on healthy subjects during dark adaptation, ambient light, and flicker stimulation and analyzed the responses in the individual capillary plexuses in the macula.

Methods

This was a prospective study that recruited healthy subjects in the Department of Ophthalmology at Northwestern University in Chicago, Illinois, between December 2017 and February 2018. This study followed the tenets of the Declaration of Helsinki, was performed in accordance with the Health Insurance Portability and Accountability Act regulations, and was approved by the Institutional Review Board of Northwestern University. Healthy volunteers were recruited to participate in the study and written informed consent was obtained from all participants. Exclusion criteria included ocular disease, media or lens opacities, and refractive error greater than ±7.0 diopters. We also excluded subjects with systemic diseases that could affect retinal circulation, such as diabetes mellitus and hypertension.

Optical Coherence Tomography Angiographic Imaging

We acquired 3 × 3-mm^2 OCTA scans centered on the fovea using the RTVue-XR Avanti system (Optovue, Inc., Fremont, CA, USA), which incorporates split-spectrum amplitude-decorrelation angiography (SSADA) software.[32] The OCTA device uses a light source centered on 840 nm with a full width at half-maximum bandwidth of 45 nm and an A-scan rate of 70,000 scans per second. The system captures two consecutive B-scans (M-B frames) at each location on the retina, with each B-scan containing 304 A-scans, and uses an orthogonal registration algorithm to reduce motion artifacts and improve the signal-to-noise ratio.[33] The SSADA algorithm extracts angiographic flow information by quantifying the OCT reflectance decorrelation between two consecutive B-scans. Only images with quality (Q-score) of 7 or greater (manufacturer's recommendation) and without large movement or shadow artifacts were considered eligible for further analysis.

Imaging Protocol

In the first experiment, 15 healthy subjects underwent dark adaptation in one eye by wearing a thick eye patch over the left eye for 45 minutes in a dimly lit room. Prior to removing the eye patch, the room was completely dark except for the OCTA computer monitor, which was adjusted to display only red light. We then removed the patch and scanned the macula four times while the eye was dark adapted, refocusing the device every two scans. The lights in the room were turned on to ambient levels (800 candela [cd]/m^2) and after 5 minutes, we reimaged the eye four more times with OCTA. We focused the OCTA on the retina following the final ambient light scan to ensure rapid imaging following flicker stimulation. The left eye was then subjected to 20 seconds of flicker stimulation using a flashing light-emitting diode (LED) light placed at the fixation light, using parameters of 10 Hz (100% contrast), 110 μW maximum power, and white light spectrum of 400 to 700 nm to stimulate the entire posterior pole. We scanned the macula immediately following the flicker stimulation, and then repeated the flicker stimulation for two more flicker-stimulated OCTA images.

In a second experiment of 10 healthy subjects, we quantified OCTA parameters during the transition from dark adaptation to ambient light. Subjects first underwent dark adaptation as described above, followed by a single OCTA scan during dark adaptation. We refocused the OCTA on the retina following the dark-adapted eye scan to ensure rapid imaging in light. Single OCTA images were taken at four different time points (at 50 seconds and at 2, 5, and 15 minutes) after the light in the room was turned to ambient levels.

Image Analysis

Two graders (P.L.N. and A.E.F.) collaboratively chose scans from each time point (dark, light, and flicker) from the first experiment that fit the inclusion criteria: Q-score of 7 or greater, lack of shadowing and motion artifact, and capillary continuity. In the second experiment, we imaged patients only once at each time point (one dark-adapted and four dark-to-light transition time points) and all images met the inclusion criteria. Therefore, in the second experiment, we used a single image per patient at each time point to calculate the following OCTA parameters. Using the built-in AngioVue Analytics software (version 2017.1.0.151) with projection artifact removal (PAR), we segmented the SCP, MCP, and DCP as previously described (Figs. 1B, 1D).[34] Briefly, the SCP was segmented from the internal limiting membrane (ILM) to 10 μm above the inner plexiform layer (IPL) to encompass the nerve fiber and ganglion cell layers. The MCP was segmented from 10 μm above to 30 μm below the IPL to encompass IPL. The DCP was segmented from 30 μm below the IPL to 10 μm below the outer plexiform layer (OPL) to encompass the OPL. For thresholding, we segmented the full retinal thickness OCTA from the ILM to 10 μm below the OPL (Fig. 1A).

We used AngioVue Analytics software to obtain parafoveal vessel density for the SCP, MCP, and DCP. The "parafovea" was defined as an annulus centered on the fovea with inner and outer ring diameters of 1 and 3 mm, respectively. Vessel density was calculated as the percentage of the parafovea occupied by retinal blood vessels (Fig. 2A).

We then exported the SCP, MCP, and DCP angiograms with the highest Q-score and least motion artifacts in the first experiment and all images from the second experiment into ImageJ (developed by Wayne Rasband, National Institutes of Health, Bethesda, MD; http://rsb.info.nih.gov/ij/index.html, in the public domain) to calculate the parafoveal adjusted flow index (AFI). AFI is an indirect and relative measure of flow velocity based on pixel intensity, which is related to flow velocity within a limited range in OCTA. Two independent graders (P.L.N. and A.E.F.) obtained these measurements through a global threshold as previously described (Figs 2B, 2C).[35,36] We also calculated the vessel length density (VLD) for the SCP to eliminate the influence of larger arterioles and venules on the density measurement (Fig. 2D).[37,38] For VLD,

Investigative Ophthalmology & Visual Science

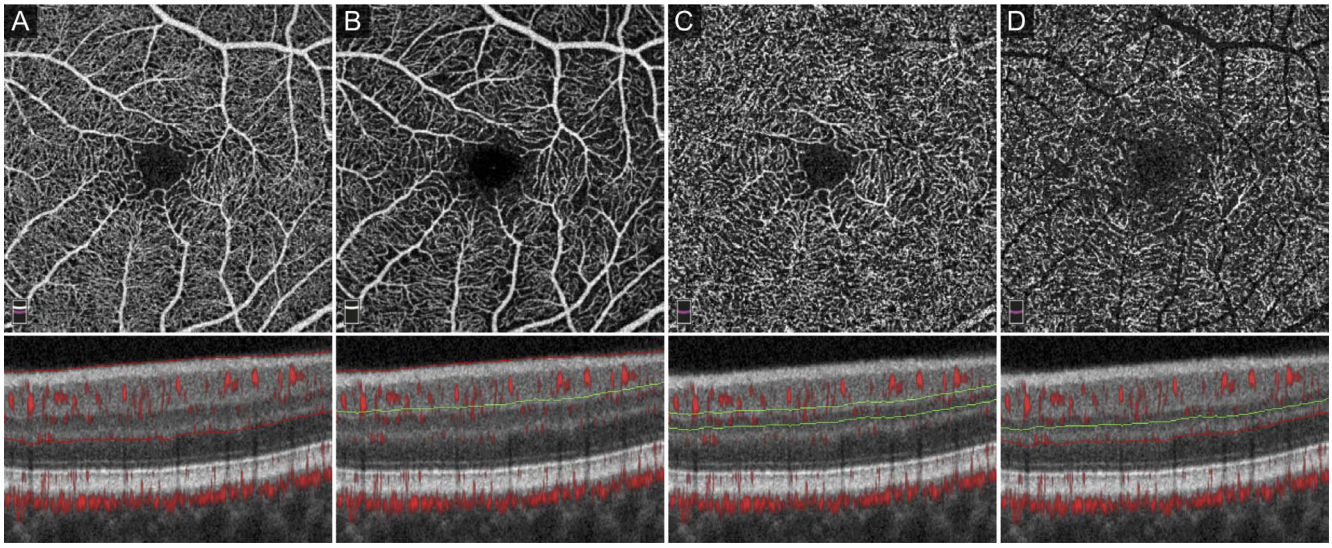

Figure 1. Segmentation of three retinal capillary plexuses in optical coherence tomography angiography. *Top row*: 3 × 3-mm^2 en face OCTA. *Bottom row*: cross-sectional OCTA with red and green segmentation boundaries and red flow overlay. (**A**) Full retinal thickness, (**B**) superficial capillary plexus, (**C**) middle capillary plexus, and (**D**) deep capillary plexus.

we binarized and skeletonized the parafoveal SCP angiogram and used the following equation to obtain VLD in units of mm^{-1}: skeletonized vessel length (mm) / parafoveal area (mm^2).

Image Subtraction

The OCTA scans with the highest Q-score and least motion artifacts from each plexus (SCP, MCP, and DCP) in the first experiment were aligned between conditions using ImageJ plug-in bUnwarpJ, an algorithm for elastic image registration.[39] All images were then cropped equally to eliminate missing areas along the borders of the images due to the aligning process. Images were then subtracted and the average pixel intensity from the resulting image was obtained for "light minus dark," "flicker minus dark," and "flicker minus light" (Fig. 3). A positive value (bright pixel) indicates more visible vessels in the first image compared to the image used to subtract, which could indicate dilation, increased flow velocity, or recruitment of vessels. A negative value (dark pixel) indicates more visible vessels in the image used to subtract compared to the first image. The means for each subtraction condition were calculated. We did not perform image alignment or subtraction for the second experiment.

Statistics

We performed initial statistical tests with SPSS version 21 (IBM SPSS Statistics; IBM Corporation, Chicago, IL, USA). A 2-way random intraclass correlation coefficient (ICC) was used to assess intergrader reliability for AFI measurements. For image subtraction, the mean values for each plexus were compared to zero using paired samples *t*-tests. No adjustments for age, refractive error, or image quality were performed for the subtraction results. A *P* value of less than 0.05 was considered statistically significant. We found moderate to strong linear Pearson correlations between vessel density and Q-score. Therefore, further statistical analyses were performed using SAS software version 9.4 (SAS Institute, Inc., Cary, NC, USA). To assess the differences in vessel density, AFI, and VLD between conditions, we performed adjusted models that included age, refractive error, and Q-score as potential confounders. For AFI and VLD analyses, we included only the best-quality scan for each condition per subject, resulting in a total of 15 scans from each condition (dark, light, and flicker). For vessel density measurements, we included all scans that met our inclusion criteria, resulting in multiple scans in each condition per subject. Therefore, the mean differences in vessel density for each plexus were assessed using mixed effect linear regression models controlling for the potential correlations from multiple

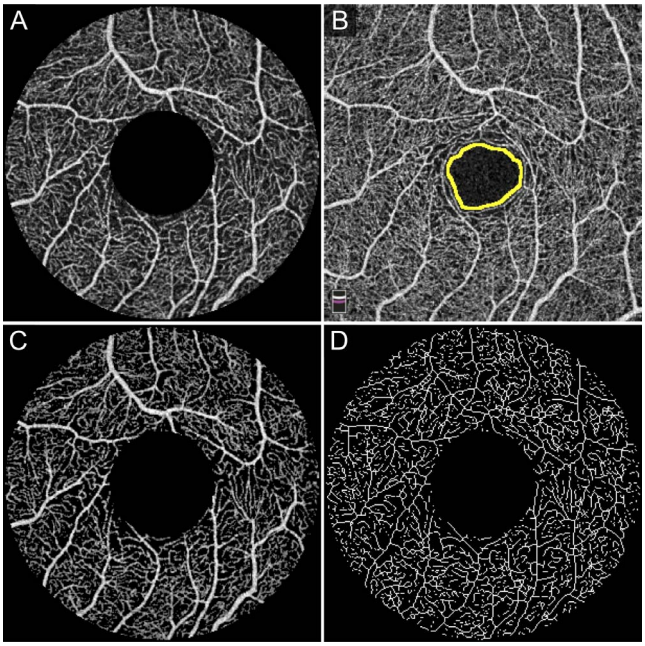

Figure 2. Optical coherence tomography angiography parameters. (**A**) 3 × 3-mm^2 en face OCTA of the superficial capillary plexus (SCP) parafovea. (**B**) Full retinal thickness OCTA with *yellow circle* delineating the foveal avascular zone used to establish the noise threshold. (**C**) OCTA of the SCP parafovea with elimination of pixels below the threshold. Average pixel intensity above the threshold was used to calculate adjusted flow index (AFI). (**D**) Binarized and skeletonized vessels of the SCP parafovea used to calculate vessel length density (VLD).

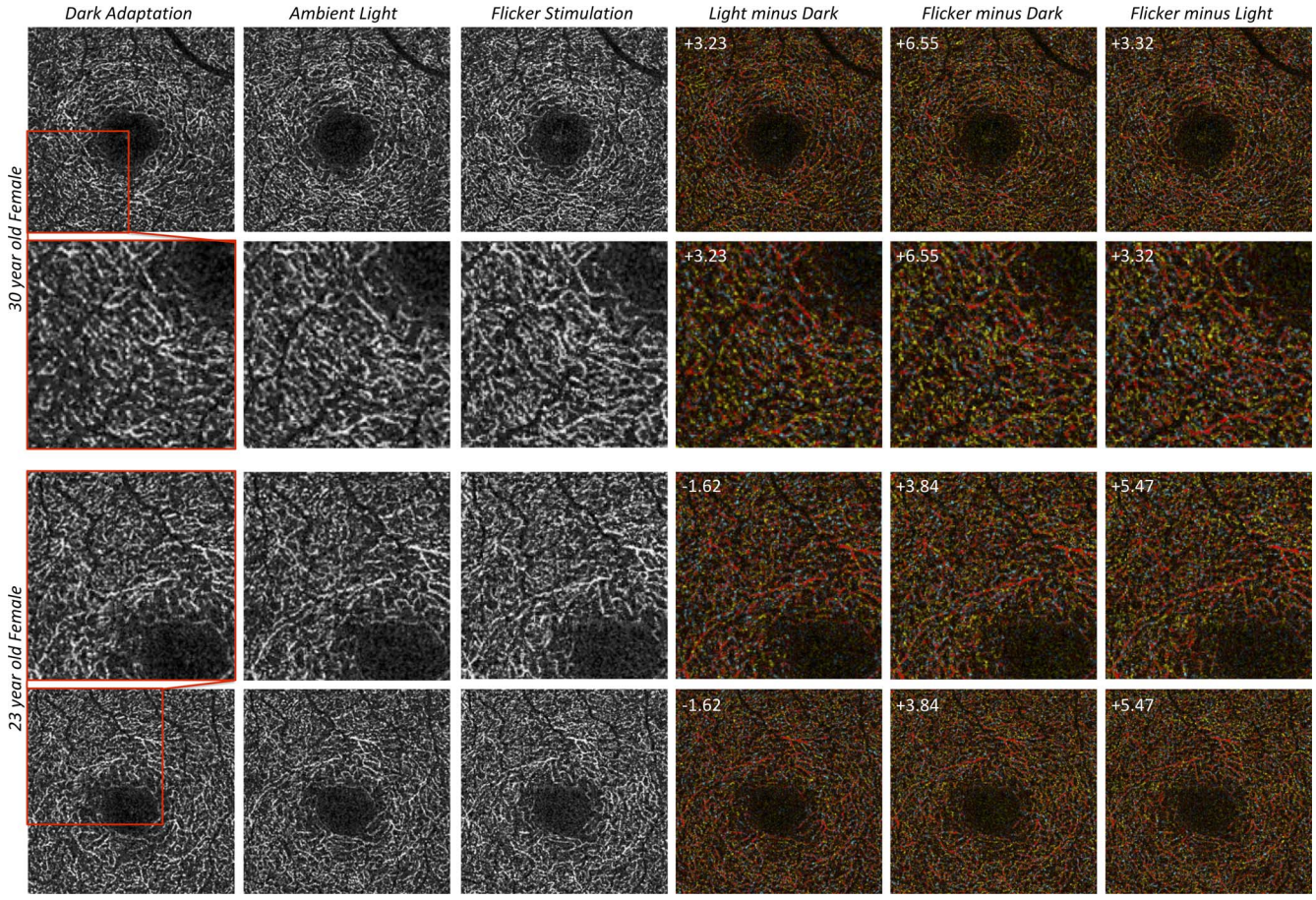

Figure 3. Image alignment and subtraction between dark adaptation, ambient light, and flicker stimulation. *Left three columns* show original optical coherence tomography angiography after aligning and cropping. *Right three columns* display pseudo-colored results from subtraction between conditions with average pixel intensity after subtraction in *upper left corner*. All images are of the deep capillary plexus. *Red* pixels represent vessels or decorrelation intensities (blood flow) that did not change between the two conditions. *Cyan* pixels represent blood flow present only in the condition used to subtract, and *yellow* pixels represent blood flow present only in the condition being subtracted from. For example, in light minus dark the *cyan* pixels represent flow present in dark adaptation but not in ambient light, *yellow* pixels are blood flow present in ambient light but not in dark adaptation, and *red* pixels are blood flow present in both. *Top row* is from a 30-year-old female and *bottom row* is from a 23-year-old female. *Middle rows* are enlarged insets of the area in within the *red boxes*.

measurements nested within each condition in the same subject. For the second experiment, we used a single OCTA image for each time point to assess the differences in vessel density, AFI, and VLD between conditions using a mixed effect linear regression model to adjust for potential confounding variables, including age, refractive error. and Q-score.

Results

From the original 17 eyes of 17 participants in the first experiment, 1 eye was excluded due to media opacities (i.e., floaters and shadow artifact on OCTA) and 1 eye was excluded due to low Q-scores (i.e., Q < 7), leaving 15 eyes of 15 healthy subjects (age 29.1 ± 8.3 years; 6 females [40%]) for the final analysis. A total of 57 dark adaptation scans, 54 ambient light scans, and 35 flicker stimulation scans fit the inclusion criteria and were used in the adjusted logistic regression model for vessel density. Only the highest-quality scan, based on Q-score and motion artifact, from each condition for each patient was used in the VLD, AFI, and image subtraction analyses.

After adjusting for age, refractive error, and Q-score, the SCP vessel density was significantly higher in ambient light ($P = 0.029$) and flicker stimulation ($P < 0.001$) compared to dark adaptation (Table 1; Fig. 4A). In contrast, SCP VLD was significantly lower in ambient light ($P = 0.011$) and flicker stimulation ($P = 0.005$) compared to dark adaptation (Table 1; Fig. 4B). MCP vessel density was significantly lower in ambient light compared to dark adaptation ($P = 0.048$; Table 1; Fig 4C). None of the other comparisons for vessel density were statistically significant, although there was a trend of increased vessel density in the SCP and DCP during flicker stimulation compared to ambient light (Table 1; Figs. 4A, 4D).

Parafoveal AFI showed good intergrader reliability with an ICC (95% confidence interval) of 0.988 (0.984–0.991). We found no statistically significant difference in AFI for any comparison (Table 1). After image alignment and subtraction, we found a positive mean value for "flicker minus dark" and "flicker minus light" in the DCP, suggesting either more dilated vessels, increased flow velocity, or recruitment of vessels in this layer during flicker stimulation compared to either dark adaptation ($P = 0.036$) or ambient light ($P = 0.007$; Table 2).

Ten eyes of 10 healthy subjects (age 29.3 ± 5.7 years; 5 females [50%]) were included in experiment 2 during the transition from dark adaptation to ambient light. After adjusting for age, refractive error, and Q-score, the SCP vessel density was significantly increased at 50 seconds of ambient light exposure compared to dark adaptation ($P = 0.013$; Fig. 5A).

Investigative Ophthalmology & Visual Science

Table 1. Parafoveal Optical Coherence Tomography Angiography Vessel Parameters in Dark Adaptation, Ambient Light, and Flicker Stimulation

	Stimulus			Pairwise Comparisons *P* Values		
OCTA Parameter	Dark Adaptation	Ambient Light	Flicker Stimulation	Dark vs. Light	Dark vs. Flicker	Light vs. Flicker
Quality score, mean ± SD	8.11 ± 0.79	8.41 ± 0.63	8.23 ± 0.69	0.082	0.164	0.334
SCP VLD, mm^{-1}, mean ± SE	14.35 ± 0.11	14.01 ± 0.16	13.81 ± 0.17	0.011*	0.005*	0.786
SCP vessel density, %, mean ± SE	49.04 ± 0.23	49.99 ± 0.22	50.31 ± 0.32	0.029*	<0.001*	0.155
MCP vessel density, %, mean ± SE	46.23 ± 0.25	45.06 ± 0.23	44.97 ± 0.25	0.048*	0.074	0.938
DCP vessel density, %, mean ± SE	44.01 ± 1.15	42.75 ± 1.62	43.16 ± 1.31	0.439	0.954	0.529
SCP AFI, mean ± SE	0.4292 ± 0.0027	0.4314 ± 0.0030	0.4321 ± 0.0035	0.969	0.825	0.790
MCP AFI, mean ± SE	0.4466 ± 0.0040	0.4451 ± 0.0038	0.4454 ± 0.0051	0.488	0.623	0.824
DCP AFI, mean ± SE	0.4305 ± 0.0048	0.4376 ± 0.0057	0.4359 ± 0.0064	0.960	0.978	0.936

* Statistical significance (*P* value of less than 0.05).

MCP vessel density was significantly lower at 50 seconds ($P = 0.002$) and 2 minutes ($P = 0.038$) of ambient light exposure compared to dark adaptation (Fig. 5B). DCP vessel density was significantly lower at 50 seconds ($P < 0.001$), 2 minutes ($P < 0.001$), 5 minutes ($P < 0.001$), and 15 minutes ($P = 0.039$) of ambient light exposure compared to dark adaptation (Fig. 5C). In each layer, the change in vessel density was most pronounced between dark adaptation and the first ambient light time point (50 seconds), followed by a more progressive descent or ascent back toward the dark adaptation value. VLD in the SCP was not significantly different for any time point. Each layer showed a trend of increased AFI during the transition from dark adaptation to ambient light, but only the SCP ($P = 0.035$) and MCP ($P = 0.011$) were significantly higher at 5 minutes of ambient light exposure compared to dark adaptation (Table 3).

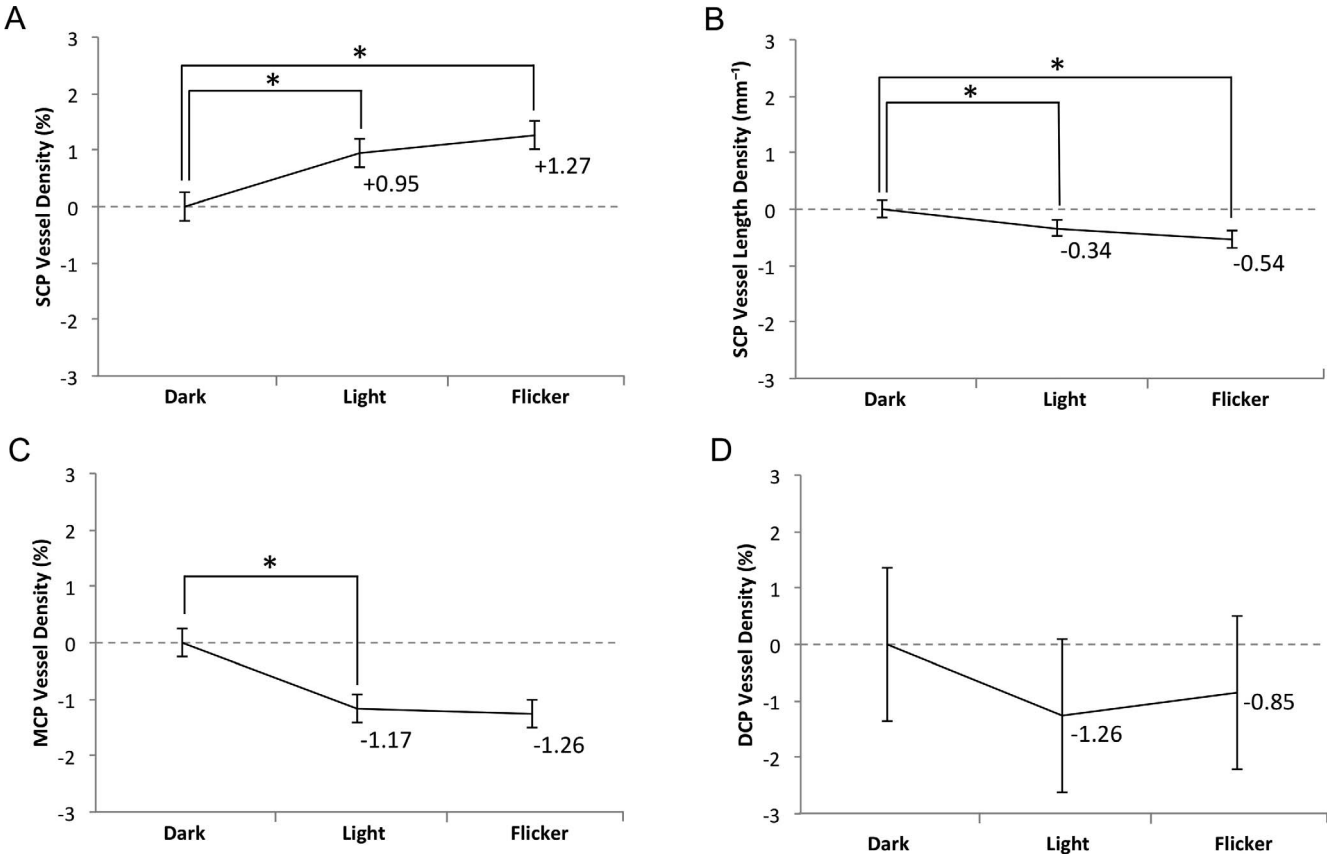

Figure 4. Parafoveal vessel density changes in optical coherence tomography angiography during dark adaptation and flicker stimulation. (**A**) Vessel density (%) in the superficial capillary plexus (SCP) was higher during ambient light (49.99 ± 0.22%) and flicker stimulation (50.31 ± 0.32%) compared to dark adaptation (49.04 ± 0.23%). For visualization, changes were normalized to dark adaptation value, which was set to zero. (**B**) Vessel length density (VLD) was lower in the SCP during ambient light (14.01 ± 0.16 mm^{-1}) and flicker stimulation (13.81 ± 0.17 mm^{-1}) compared to dark adaptation (14.35 ± 0.11 mm^{-1}). (**C**) Vessel density (%) in the middle capillary plexus (MCP) was significantly lower during ambient light (45.06 ± 0.23%) compared to dark adaptation (46.23 ± 0.25%). (**D**) Vessel density (%) in the deep capillary plexus (DCP) was not significantly different during any condition. There was a trend of increasing vessel density in the SCP and DCP during flicker stimulation compared to ambient light, although this did not reach statistical significance in either layer (**A**, **D**). *Error bars* represent standard errors. *Asterisks* represent a *P* value of less than 0.05.

Table 2. Average Image Subtraction Results Between Dark Adaptation, Ambient Light, and Flicker Stimulation

Capillary Plexus	Light Minus Dark	Flicker Minus Dark	Flicker Minus Light
SCP	1.02	0.60	−0.42
MCP	−0.42	0.56	0.71
DCP	−0.22	1.79*	2.02*

Optical coherence tomography angiography reveals significantly more vessels in the deep capillary plexus during flicker stimulation compared to either dark adaptation or ambient light.

* Statistical significance (*P* value of less than 0.05).

Discussion

In this study, we used OCTA to measure parafoveal vessel density, VLD, and AFI while adjusting for age, refractive error, and scan quality in healthy subjects during dark adaptation, the transition from dark to ambient light, and after flicker stimulation. We found a significant increase in SCP vessel density and decrease in SCP skeletonized density (VLD) during ambient light and flicker stimulation compared to dark adaptation. We also found a significant decrease in MCP vessel density during ambient light compared to dark adaptation. After image alignment and subtraction, we found a statistically significant positive mean value for DCP "flicker minus dark" and "flicker minus light," suggesting more open or dilated vessels during flicker stimulation, although we did not adjust for covariables in this analysis. During the transition from dark to ambient light, we also found a transient significant increase in SCP vessel density (50 seconds) along with more persistent decrease in the deeper capillaries, continuing up to 2 minutes in the MCP and 15 minutes in the DCP.

The human parafovea is supplied by an interconnected, complex trilaminar vascular network. In the nerve fiber and ganglion cell layers, large arterioles and venules branch into the capillaries of the SCP, and also provide branches that supply and drain the capillary beds of the MCP and DCP.[28] These three capillary plexuses are also interconnected via vertical capillary anastomoses.[40] The VLD used in this study measures vessel density of the skeletonized en face OCTA image. Skeletonization converts all blood vessels into 1-pixel-wide lines on the angiogram, thus removing any extra weight afforded to larger vessels in the SCP. Thus, VLD preferentially measures changes in small capillaries that are near the threshold of OCTA detection. In contrast, large vessels are disproportionately represented in the standard vessel density (%) measurements. Numerous studies have shown an increase in large vessel flow velocity and vessel diameter during flicker stimulation.[16–26] In our study, the increase in vessel density and decrease in VLD in the SCP during ambient light and flicker stimulation suggest active dilation of the larger vessels and redistribution of blood from the smaller capillaries to either the larger SCP vessels or toward the deeper layers via anastomoses, which are vertically oriented (parallel to the OCT beam) and may therefore be difficult to detect with OCTA.[28]

In contrast to SCP vessel density (Fig. 4A), we found the opposite trend in the MCP (Fig. 4C), which was decreased significantly during ambient light compared to dark adaptation, and not significantly during flicker stimulation. During the transition from dark to light, this difference was more pronounced with significantly increased SCP density and decreased MCP and DCP density compared to dark adaptation (Fig. 5). These vascular changes appeared to be transient, especially in the SCP, with the greatest change occurring in the first 50 seconds. Of the deeper layers, only the DCP remained significantly decreased up to 15 minutes. These findings suggest that the DCP is maximally dilated during dark adaptation, then rapidly constricts during the transition from dark to light allowing the blood flow to be redirected to the more superficial layers. Alternatively, the dilation of the larger SCP vessels in ambient light could mask the OCTA signal from deeper layers due to shadowing effects, which could potentially explain the reduction in MCP and DCP vessel density during the transition from dark to light. We also recognize that the changes in DCP vessel density during ambient light compared to dark adaptation seen in the second experiment were more significant compared to the first experiment. This could be attributed to the difference in the number of images acquired between the two experiments. In the first experiment, we acquired four dark-adapted images followed by four ambient light images and included all the images that met our inclusion criteria for statistical analysis. In the second experiment, we acquired a single dark-adapted image followed by ambient light images at 50 seconds and at 2, 5, and 15 minutes, using a single OCTA image for each time point in the

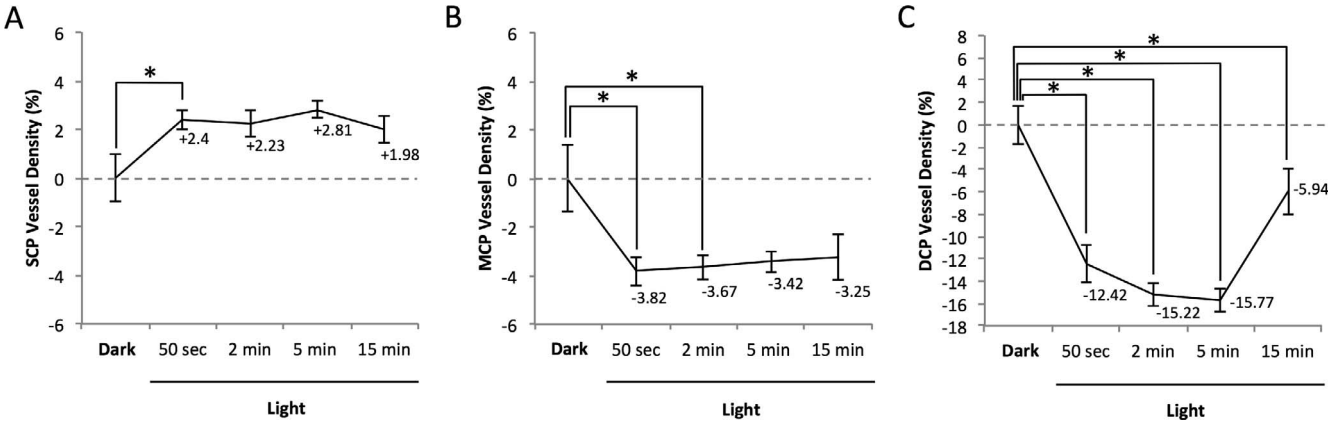

Figure 5. Parafoveal vessel density changes in optical coherence tomography angiography during transition from dark adaptation to ambient light. (**A**) Vessel density (%) in the superficial capillary plexus (SCP) was significantly increased at 50 seconds of ambient light exposure (50.11 ± 0.40%) compared to dark adaptation (47.71 ± 0.96%). For visualization, changes were normalized to dark adaptation value, which was set to zero. (**B**) Middle capillary plexus (MCP) vessel density was significantly lower at 50 seconds (43.64 ± 0.59%) and 2 minutes (43.79 ± 0.49%) of ambient light exposure compared to dark adaptation (47.46 ± 1.39%). (**C**) Deep capillary plexus (DCP) vessel density was significantly lower at 50 seconds (38.86 ± 1.69%), 2 minutes (36.06 ± 1.08%), 5 minutes (35.51 ± 1.00%), and 15 minutes (45.34 ± 2.08%) of ambient light exposure compared to dark adaptation (51.28 ± 1.74%). *Error bars* represent standard errors. *Asterisks* represent a *P* value less than 0.05.

Investigative Ophthalmology & Visual Science

Investigative Ophthalmology & Visual Science

Table 3. Parafoveal Optical Coherence Tomography Angiography Vessel Parameters During Transition From Dark Adaptation to Ambient Light

OCTA Parameter	Dark Adaptation	Ambient Light				Pairwise Comparisons *P* Values			
		50 s	2 min	5 min	15 min	Dark vs. 50 s	Dark vs. 2 min	Dark vs. 5 min	Dark vs. 15 min
SCP VLD, mm^{-1}, mean ± SE	22.43 ± 0.41	23.31 ± 0.16	22.82 ± 0.23	22.33 ± 0.25	22.75 ± 0.15	0.063	0.924	0.192	0.766
SCP vessel density, %, mean ± SE	47.71 ± 0.96	50.11 ± 0.40	49.94 ± 0.53	50.52 ± 0.33	49.69 ± 0.55	0.013*	0.083	0.066	0.083
MCP vessel density, %, mean ± SE	47.46 ± 1.39	43.64 ± 0.59	43.79 ± 0.49	44.04 ± 0.43	44.21 ± 0.92	0.002*	0.038*	0.222	0.071
DCP vessel density, %, mean ± SE	51.28 ± 1.74	38.86 ± 1.69	36.06 ± 1.08	35.51 ± 1.00	45.34 ± 2.08	<0.001*	<0.001*	<0.001*	0.039*
SCP AFI, mean ± SE	0.3874 ± 0.0089	0.4010 ± 0.0050	0.4085 ± 0.0061	0.4202 ± 0.0041	0.3973 ± 0.0063	0.349	0.154	0.035*	0.532
MCP AFI, mean ± SE	0.3938 ± 0.0102	0.4120 ± 0.0069	0.4206 ± 0.0071	0.4389 ± 0.0056	0.3991 ± 0.0075	0.317	0.139	0.011*	0.924
DCP AFI, mean ± SE	0.3745 ± 0.0131	0.3836 ± 0.0103	0.3968 ± 0.0098	0.4227 ± 0.0068	0.3800 ± 0.0091	0.927	0.517	0.051	0.922

* Statistical significance (*P* value less than 0.05).

statistical analysis. In addition, the different imaging protocols could have altered the subjects' physiological stress responses, such as blood pressure, which was not measured in this study.

The finding of maximally dilated DCP in dark adaptation is very exciting, with important implications for pathological capillary loss in the DCP in ischemic disease states. Using OCT and adaptive optics scanning laser ophthalmoscopy, we have shown a correlation between a loss of DCP capillaries and disruption of photoreceptors in diabetic retinopathy (DR).[41,42] The current study suggests that the physiological deficit from the loss of DCP capillaries in patients with DR may be most pronounced during dark adaptation when these vessels are normally more dilated, in order to maximize oxygen delivery to the highly metabolically active dark-adapted photoreceptors, as previously shown in the animal models.[7,8] Furthermore, we have reported that OCTA parameters in the MCP and DCP change in a different direction than the SCP during the progression of DR.[35,43] We have also shown that reduced OCTA flow signal is localized to specific capillary layers in paracentral acute middle maculopathy (MCP and DCP) and acute macular neuroretinopathy (DCP).[44] The current results further confirm distinct neurovascular control mechanisms for each plexus,[45] potentially related to different neuromodulators acting on the different capillary plexuses. Nitric oxide has recently been shown to be elaborated by distinct subtypes of amacrine cells that are maximally activated by flicker stimulation, providing a potentially novel mechanism for differential neurovascular coupling at the deeper plexuses.[46]

Interestingly, while we did not find significant changes in DCP vessel density or AFI following flicker (Table 1; Fig. 4D), we uncovered a significant increase in the DCP capillary signal compared to ambient light or dark adaptation by using elastic alignment and image subtraction. This finding suggests either higher DCP blood flow or more open/dilated vessels during flicker stimulation compared to either dark adaptation or ambient light (Table 2). It is possible that the high standard error of DCP vessel density measurement is due to small movements in scan location, which may also explain the difficulty in identifying significant differences unless the images are rigorously registered (Fig. 3).

Previous reports on retinal vascular response to dark adaptation have been inconsistent. Some studies showed an increase in large retinal vessel flow velocity, vessel caliber, or both during dark adaptation,[9–11] while others reported no change.[12–15] We expected an increase in blood flow in the DCP, since this plexus is nearest the photoreceptors and supplies 10% of the photoreceptor metabolic demands in the dark.[7,8] We found that DCP vessel density was significantly greater in the dark compared to ambient light, but rapidly (50 seconds) and significantly decreased with exposure to light (Fig. 5C). When measurements were made after the transition period, these values were no longer significantly different. Riva et al.[15] found a transient increase in flow velocity in large vessels near the optic disc when transitioning to ambient light from a dark-adapted state. We found a trend for increased AFI in all layers following transition to ambient light in our study, with only the SCP and MCP reaching statistical significance at 5 minutes following ambient light exposure (Table 3). This finding could also be related to the greater standard error in the DCP measurements compared to the other plexuses (Table 1; Fig. 4D), which in turn could be attributed to signal attenuation at greater retinal depths, inherent to spectral-domain (SD) hardware. Another potential explanation could relate to artifactual excessive removal of real flow in the DCP by the relatively new PAR software (Optovue, Inc.). For example, Figure 1D reveals the negative vascular shadows produced by the PAR algorithm in the attempt to remove projection artifacts from larger overlying vessels. Dilation or

constriction of large SCP vessels that cast shadows on the DCP may be masking real changes in DCP vessel density or AFI. Future studies using different PAR software could provide further insight into the effect of dark adaptation and flicker stimulation on the DCP.

In most of the previous studies, flow velocity and vessel caliber measurements were obtained in large retinal vessels (i.e., central retinal artery/vein, branch retinal arteries, large vessels near the nerve head), while our study focused on the parafoveal vessels, mostly capillaries within the central 3 × 3 mm^2. Duan et al.[47] used flood-illuminated adaptive optics to study the hemodynamic response to flicker stimulation in the smallest vessels of the human retina (range, 3–28 μm). These authors found variable response of capillaries upon flicker stimulation, with 35% of vessels showing dilation and 7% showing constriction, with a greater proportion of arterioles dilating and venules constricting.[47] While there are a limited number of studies that report on the effects of flicker stimulation on the three capillary layers in humans, previous studies have shown the existence of superficial, middle, and deep capillaries in the rat retina.[48] Leahy et al.[40] performed OCTA and computational analyses to derive a vectorized 3D representation of the vascular architecture of the rat retina. These authors constructed simulations for the effect of dilation of interlayer anastomoses on the downstream caliber changes in each of the plexuses. Their simulation showed variable response in the surrounding capillaries, including dilation and constriction.[40] In the rat retina, Kornfield and Newman[45] found that the three plexuses were differentially regulated, with larger flicker-evoked vasodilation and greater flow velocity increase in the capillaries of the MCP compared to the SCP or DCP. These studies suggest a highly variable response to flicker stimulation at the capillary level. While the high variability in vascular response could explain the lack of statistically significant changes from ambient light to flicker in our data, it could also be attributed to the fact that we treated all vessels in the parafovea as a single entity without distinguishing between arterioles and venules. Future OCTA studies may benefit from techniques that allow researchers to better distinguish the responses in capillaries closer to arterioles or venules.

The SSADA software used in this study calculates decorrelation by analyzing OCT signal amplitude differences between two sequential B-scans from the same location on the retina.[32] OCTA decorrelation values and blood flow velocity are linearly related within a limited range (flow speeds between 0.4 and 3 mm/s for SSADA).[49] Therefore, changes in flow speeds within this range would be reflected by a linear change in AFI. In a previous OCTA study, Wei and colleagues[31] found a significant increase in full retinal thickness parafoveal flow index (based on decorrelation) during checkerboard pattern stimulation. The checkerboard pattern mimics the stimulus used in electroretinography, which measures the electrical response of retinal ganglion cells. The 10-Hz flicker used in our study likely activates retinal ganglion cells as well, but checkerboard and flicker could potentially activate different sets of inner retinal neurons.[50,51] Wei et al.[31] also used swept-source (SS)-OCTA and performed OCTA scanning simultaneous to checkerboard stimulation, while our imaging was performed subsequent to flicker stimulation. In the current study, we found no significant changes in the subplexus AFI (based on decorrelation) during flicker stimulation. The only significant finding for the AFI parameter in our study occurred at the 5-minute mark during transition from dark to ambient light and only in the SCP and MCP (Table 3). The lack of significant AFI changes during flicker stimulation in our study could be attributed to the different flicker stimulus or OCTA hardware used, or the limited range in which decorrelation and flow velocity are linearly correlated. Our lack of significant AFI data during flicker may also be attributed to the time course of imaging, as we performed OCTA scans immediately after flicker stimulation as opposed to performing OCTA scans simultaneously with flicker stimulation. Indeed, some studies have reported that retinal vessels return to baseline diameter after 10 to 40 seconds from cessation of flicker stimulation, an event that we may have missed in our imaging.[22,25]

Our study was limited by a small sample size as well as an external flicker stimulus, which did not allow for simultaneous OCTA scanning and flicker stimulation. Future studies using a built-in flicker or pattern stimulus could provide further insight into the hemodynamic response to different types of stimulation. Our study was also limited by the proprietary PAR (projection removal) algorithm, the effects of which are largely unknown, especially on OCTA parameters such as vessel density in the DCP.[34,44] Alternative algorithms, such as projection-resolution (PR)-OCTA, could be useful in future studies.[44,52–54] This study is also limited by the sensitivity of OCTA software to detect small capillaries, which has not yet been fully assessed. Furthermore, blood pressure, intraocular pressure, and other physiological variables that could affect vascular OCTA parameters were not measured in this study. Strengths of our study included adjusting for refractive error, age, and scan quality, which are known to affect OCTA parameters. This study also focuses on the less well-studied, small-caliber vessels during dark adaptation and flicker.

In summary, using OCTA, we found a significant increase in SCP vessel density and decrease in SCP skeletonized density (VLD) during ambient light and flicker stimulation compared to dark adaptation. We also found a transient increase in SCP vessel density and decrease in MCP and DCP vessel density following the transition from dark to ambient light, suggesting constriction of the DCP and MCP and a significant large vessel dilation response in the SCP. We also found a significant positive result in apparent vessel density after elastic registration, alignment, and image subtraction in the DCP, suggesting more flow or dilated capillaries in the DCP during flicker. Our study provides further evidence for neurovascular coupling in the retina under different light conditions, supporting differential regulation at the different plexuses. Future studies with larger cohorts and better software algorithms for studying the deeper capillaries are needed to provide further insight into the differential regulation of the retinal capillary plexuses in health and disease.

Acknowledgments

Supported by a National Institutes of Health grant (1DP3 DK108248; AAF) and research instrument support by Optovue, Inc., Fremont, California, United States. The authors alone are responsible for the content and writing of the paper.

Disclosure: **P.L. Nesper**, None; **H.E. Lee**, None; **A.E. Fayed**, None; **G.W. Schwartz**, None; **F. Yu**, None; **A.A. Fawzi**, None

References

1. Riva CE, Logean E, Falsini B. Visually evoked hemodynamical response and assessment of neurovascular coupling in the optic nerve and retina. *Prog Retin Eye Res*. 2005;24:183–215.
2. Riva C, Harino S, Shonat R, Petrig B. Flicker evoked increase in optic nerve head blood flow in anesthetized cats. *Neurosci Lett*. 1991;128:291–296.
3. Mandecka A, Dawczynski J, Blum M, et al. Influence of flickering light on the retinal vessels in diabetic patients. *Diabetes Care*. 2007;30:3048–3052.
4. Lim LS, Ling LH, Ong PG, Foulds W, Tai ES, Wong TY. Dynamic responses in retinal vessel caliber with flicker light stimula-

tion and risk of diabetic retinopathy and its progression. *Invest Ophthalmol Vis Sci*. 2017;58:2449–2455.

5. Wong-Riley M. Energy metabolism of the visual system. *Eye Brain*. 2010;2:99.
6. Kur J, Newman EA, Chan-Ling T. Cellular and physiological mechanisms underlying blood flow regulation in the retina and choroid in health and disease. *Prog Retin Eye Res*. 2012; 31:377–406.
7. Linsenmeier RA. Effects of light and darkness on oxygen distribution and consumption in the cat retina. *J Gen Physiol*. 1986;88:521–542.
8. Birol G, Wang S, Budzynski E, Wangsa-Wirawan ND, Linsenmeier RA. Oxygen distribution and consumption in the macaque retina. *Am J Physiol Heart Circ Physiol*. 2007;293: H1696–H1704.
9. Havelius U, Hansen F, Hindfelt B, Krakau T. Human ocular vasodynamic changes in light and darkness. *Invest Ophthalmol Vis Sci*. 1999;40:1850–1855.
10. Feke G, Zuckerman R, Green G, Weiter J. Response of human retinal blood flow to light and dark. *Invest Ophthalmol Vis Sci*. 1983;24:136–141.
11. Riva C, Grunwald J, Petrig B. Reactivity of the human retinal circulation to darkness: a laser Doppler velocimetry study. *Invest Ophthalmol Vis Sci*. 1983;24:737–740.
12. Barcsay G, Seres A, Németh J. The diameters of the human retinal branch vessels do not change in darkness. *Invest Ophthalmol Vis Sci*. 2003;44:3115–3118.
13. von Hanno T, Sjølie AK, Mathiesen EB. Retinal vascular calibre and response to light exposure and serial imaging. *Acta Ophthalmol*. 2014;92:444–448.
14. Alagöz C, Pekel G, Alagöz N, et al. Choroidal thickness, photoreceptor thickness, and retinal vascular caliber alterations in dark adaptation. *Curr Eye Res*. 2016;41:1608–1613.
15. Riva CE, Logean E, Petrig BL, Falsini B. Effet de l'adaptation à l'obscurité sur le flux rétinien. *Klin Monbl Augenheilkd*. 2000;216:309–310.
16. Nagel E, Vilser W, Lanzl I. Age, blood pressure, and vessel diameter as factors influencing the arterial retinal flicker response. *Invest Ophthalmol Vis Sci*. 2004;45:1486–1492.
17. Shih Y-YI, Wang L, De La Garza BH, et al. Quantitative retinal and choroidal blood flow during light, dark adaptation and flicker light stimulation in rats using fluorescent microspheres. *Curr Eye Res*. 2013;38:292–298.
18. Garhöfer G, Zawinka C, Resch H, Huemer K, Dorner G, Schmetterer L. Diffuse luminance flicker increases blood flow in major retinal arteries and veins. *Vision Res*. 2004;44:833–838.
19. Sharifizad M, Witkowska KJ, Aschinger GC, et al. Factors determining flicker-induced retinal vasodilation in healthy ubjects. *Invest Ophthalmol Vis Sci*. 2016;57:3306–3312.
20. Garhöfer G, Zawinka C, Huemer K-H, Schmetterer L, Dorner GT. Flicker light–induced vasodilatation in the human retina: effect of lactate and changes in mean arterial pressure. *Invest Ophthalmol Vis Sci*. 2003;44:5309–5314.
21. Wang Y, Fawzi AA, Tan O, Zhang X, Huang D. Flicker-induced changes in retinal blood flow assessed by Doppler optical coherence tomography. *Biomed Opt Express*. 2011;2:1852–1860.
22. Polak K, Schmetterer L, Riva CE. Influence of flicker frequency on flicker-induced changes of retinal vessel diameter. *Invest Ophthalmol Vis Sci*. 2002;43:2721–2726.
23. Noonan JE, Nguyen TT, Man RE, Best WJ, Wang JJ, Lamoureux EL. Retinal arteriolar dilation to flicker light is reduced on short-term retesting. *Invest Ophthalmol Vis Sci*. 2013;54: 7764–7768.
24. Hammer M, Vilser W, Riemer T, et al. Retinal venous oxygen saturation increases by flicker light stimulation. *Invest Ophthalmol Vis Sci*. 2011;52:274–277.
25. Felder AE, Wanek J, Blair NP, Shahidi M. Retinal vascular and oxygen temporal dynamic responses to light flicker in humans. *Invest Ophthalmol Vis Sci*. 2017;58:5666–5672.
26. Son T, Wang B, Thapa D, et al. Optical coherence tomography angiography of stimulus evoked hemodynamic responses in individual retinal layers. *Biomed Opt Express*. 2016;7:3151–3162.
27. Chan G, Balaratnasingam C, Paula KY, et al. Quantitative morphometry of perifoveal capillary networks in the human retina. *Invest Ophthalmol Vis Sci*. 2012;53:5502–5514.
28. Nesper PL, Fawzi AA. Human parafoveal capillary vascular anatomy and connectivity revealed by optical coherence tomography angiography. *Invest Ophthalmol Vis Sci*. 2018; 59:3858–3867.
29. Park JJ, Soetikno BT, Fawzi AA. Characterization of the middle capillary plexus using optical coherence tomography angiography in healthy and diabetic eyes. *Retina*. 2016;36:2039–2050.
30. Hwang TS, Zhang M, Bhavsar K, et al. Visualization of 3 distinct retinal plexuses by projection-resolved optical coherence tomography angiography in diabetic retinopathy. *JAMA Ophthalmol*. 2016;134:1411–1419.
31. Wei E, Jia Y, Tan O, et al. Parafoveal retinal vascular response to pattern visual stimulation assessed with OCT angiography. *PLoS One*. 2013;8:e81343.
32. Jia Y, Tan O, Tokayer J, et al. Split-spectrum amplitude-decorrelation angiography with optical coherence tomography. *Opt Express*. 2012;20:4710–4725.
33. Kraus MF, Liu JJ, Schottenhamml J, et al. Quantitative 3D-OCT motion correction with tilt and illumination correction, robust similarity measure and regularization. *Biomed Opt Express*. 2014;5:2591–2613.
34. Zhou Q. New Angiovue® Software Streamlines OCTA Interpretation. *Optical Coherence Tomography Angiography (OCTA) Quantification through AngioAnalytics™*. Available at: https://www.haag-streit.com/fileadmin/Haag-Streit_UK/Downloads/Optovue_downloads/AngioVue_downloads/AngioAnalytics_Scientific_Article_Compendium_2017.pdf. Accessed January 31, 2019.
35. Nesper PL, Roberts PK, Onishi AC, et al. Quantifying microvascular abnormalities with increasing severity of diabetic retinopathy using optical coherence tomography angiography. *Invest Ophthalmol Vis Sci*. 2017;58:BIO307–BIO315.
36. Alten F, Heiduschka P, Clemens CR, Eter N. Exploring choriocapillaris under reticular pseudodrusen using OCT-angiography. *Graefes Arch Clin Exp Ophthalmol*. 2016;254: 2165–2173.
37. Zheng D, LaMantia A-S, Purves D. Specialized vascularization of the primate visual cortex. *J Neurosci*. 1991;11:2622–2629.
38. Tam J, Martin JA, Roorda A. Noninvasive visualization and analysis of parafoveal capillaries in humans. *Invest Ophthalmol Vis Sci*. 2010;51:1691–1698.
39. Sorzano COS, Thévenaz P, Unser M. Elastic registration of biological images using vector-spline regularization. *IEEE Trans Biomed Eng*. 2005;52:652–663.
40. Leahy C, Radhakrishnan H, Weiner G, Goldberg JL, Srinivasan VJ. Mapping the 3D connectivity of the rat inner retinal vascular network using OCT angiography. *Invest Ophthalmol Vis Sci*. 2015;56:5785–5793.
41. Scarinci F, Nesper PL, Fawzi AA. Deep retinal capillary nonperfusion is associated with photoreceptor disruption in diabetic macular ischemia. *Am J Ophthalmol*. 2016;168:129–138.
42. Nesper PL, Scarinci F, Fawzi AA. Adaptive optics reveals photoreceptor abnormalities in diabetic macular ischemia. *PLoS One*. 2017;12:e0169926.

Investigative Ophthalmology & Visual Science

43. Onishi AC, Nesper PL, Roberts PK, et al. Importance of considering the middle capillary plexus on OCT angiography in diabetic retinopathy. *Invest Ophthalmol Vis Sci*. 2018;59:2167–2176.
44. Chu S, Nesper PL, Soetikno BT, Bakri SJ, Fawzi AA. Projection-resolved OCT angiography of microvascular changes in paracentral acute middle maculopathy and acute macular neuroretinopathy. *Invest Ophthalmol Vis Sci*. 2018;59:2913–2922.
45. Kornfield TE, Newman EA. Regulation of blood flow in the retinal trilaminar vascular network. *J Neurosci*. 2014;34:11504–11513.
46. Jacoby J, Nath A, Jessen ZF, Schwartz GW. A self-regulating gap junction network of amacrine cells controls nitric oxide release in the retina. *Neuron*. 2018;100:1149–1162.
47. Duan A, Bedggood PA, Bui BV, Metha AB. Evidence of flicker-induced functional hyperaemia in the smallest vessels of the human retinal blood supply. *PLoS One*. 2016;11:e0162621.
48. Genevois O, Paques M, Simonutti M, et al. Microvascular remodeling after occlusion-recanalization of a branch retinal vein in rats. *Invest Ophthalmol Vis Sci*. 2004;45:594–600.
49. Tokayer J, Jia Y, Dhalla A-H, Huang D. Blood flow velocity quantification using split-spectrum amplitude-decorrelation angiography with optical coherence tomography. *Biomed Opt Express*. 2013;4:1909–1924.
50. Werblin FS, Dowling JE. Organization of the retina of the mudpuppy, Necturus maculosus. II. Intracellular recording. *J Neurophysiol*. 1969;32:339–355.
51. Newman EA. Functional hyperemia and mechanisms of neurovascular coupling in the retinal vasculature. *J Cereb Blood Flow Metab*. 2013;33:1685–1695.
52. Campbell J, Zhang M, Hwang T, et al. Detailed vascular anatomy of the human retina by projection-resolved cptical coherence tomography angiography. *Sci Rep*. 2017;7:42201.
53. Zhang M, Hwang TS, Campbell JP, et al. Projection–resolved optical coherence tomographic angiography. *Biomed Opt Express*. 2016;7:816–828.
54. Nesper PL, Soetikno BT, Treister AD, Fawzi AA. Volume-rendered projection-resolved OCT angiography: 3D lesion complexity is associated with therapy response in wet age-related macular degeneration. *Invest Ophthalmol Vis Sci*. 2018;59:1944–1952.

Investigative Ophthalmology & Visual Science